Published in final edited form as:
Arch Biochem Biophys. 2011 July ; 511(1-2): 107–117. doi:10.1016/j.abb.2011.05.002.

Functional Asymmetry for the Active Sites of Linked 5-Aminolevulinate Synthase and 8-Amino-7-Oxononanoate Synthase

Tracy D. Turbeville[*], **Junshun Zhang**[*], **W. Christopher Adams**[*], **Gregory A. Hunter**[*], and **Gloria C. Ferreira**[*,†,‡]

[*] Department of Molecular Medicine, College of Medicine, University of South Florida, Tampa, Florida, 33612

[†] H. Lee Moffitt Cancer Center and Research Institute, University of South Florida, Tampa, Florida, 33612

[‡] Department of Chemistry, University of South Florida, Tampa, Florida, 33612

Abstract

5-Aminolevulinate synthase (ALAS) and 8-amino-7-oxononanoate synthase (AONS) are homodimeric members of the α-oxoamine synthase family of pyridoxal 5′-phosphate (PLP)-dependent enzymes. Previously, linking two ALAS subunits into a single polypeptide chain dimer yielded an enzyme (ALAS/ALAS) with a significantly greater turnover number than that of wild-type ALAS. To examine the contribution of each active site to the enzymatic activity of ALAS/ALAS, the catalytic lysine, which also covalently binds the PLP cofactor, was substituted with alanine in one of the active sites. Albeit the chemical rate for the pre-steady-state burst of ALA formation was identical in both active sites of ALAS/ALAS, the k_{cat} values of the variants differed significantly (4.4 ± 0.2 min^{-1} *vs.* 21.6 ± 0.7 min^{-1}) depending on which of the two active sites harbored the mutation. We propose that the functional asymmetry for the active sites of ALAS/ALAS stems from linking the enzyme subunits and the introduced intermolecular strain alters the protein conformational flexibility and rates of product release. Moreover, active site functional asymmetry extends to chimeric ALAS/AONS proteins, which while having a different oligomeric state, exhibit different rates of product release from the two ALAS and two AONS active sites due to the created intermolecular strain.

Keywords

5-Aminolevulinate; 5-aminolevulinate synthase; 8-amino-7-oxononanoate synthase; pyridoxal 5′ phosphate; α-oxoamine synthase family

1. INTRODUCTION

Pyridoxal 5′-phosphate (PLP) is a necessary cofactor for a large and catalytically versatile family of enzymes classified according to structural and mechanistic homologies [1–5]. The α-oxoamine synthases are a small but metabolically important subfamily within fold-type I PLP-dependent enzymes and include 5-aminolevulinate synthase (ALAS), 8-amino-7-oxononanoate synthase (AONS), serine palmitoyltransferase (SPT), and 2-amino-3-

Correspondence should be addressed to: Gloria C. Ferreira, Department of Molecular Medicine, College of Medicine, MDC 7, University of South Florida, 12901 Bruce B. Downs Blvd., Tampa, FL, 33612, Tel. (813) 974-5797, Fax: (813) 974-0504, gferreir@health.usf.edu.

oxobutyrate CoA ligase [6–13]. The catalytic cores of these four enzymes share approximately 12% overall amino acid sequence identity, while the identity between any pair is near 30% [10]. The three-dimensional structures of the α-oxoamine synthases are also highly conserved, as demonstrated by the C^{α} root-mean-square deviation values for SPT of 1.4–1.6 Å relative to the other three members [7]. Recently, two new members, CqsA [14] and LqsA [15,16], joined the α-oxoamine synthase subfamily. While both synthesize α-hydroxyketone signaling molecules with major roles in quorum sensing [17], the autoinducer synthase CqsA produces the cholera autoinducer-1 (CAI-1)[14] and the autoinducer synthase LqsA synthesizes the *Legionella* autoinducer-1 (LAI-1) [15–17].

ALAS and AONS catalyze very similar reactions, namely the Claisen-type condensation between a small amino acid and acyl-CoA thioester, with concomitant decarboxylation of the amino acid, leading to the formation of a 1-2-aminoketone product, CoA, and carbon dioxide [3,10]. ALAS catalyzes the reaction between glycine and succinyl-CoA to give ALA, whereas AONS catalyzes the mechanistically analogous reaction between alanine and pimeloyl-CoA to yield 8-amino-7-oxononanoate (AON) (Scheme 1). Both ALA and AON are essential metabolic compounds: the first is the universal precursor to tetrapyrolles, [3,18] and the second is an intermediate in biotin synthesis [19].

ALAS and AONS function as homodimers [8,10,18]. The active sites are located at the subunit interface, where the PLP cofactor is covalently bound to a conserved lysine residue through a Schiff base linkage [8,10,20]. Each monomer consists of three domains, a short N-terminal domain (~50 residues), a central catalytic domain (~250 residues), and a C-terminal domain (~100 residues). Although all three domains participate in dimerization, the catalytic domain contributes the most to the dimeric interface [7,8,10]. Shared active sites at the intersubunit interface of dimeric proteins elicit major questions about the roles of residues from either subunit toward the activity of the enzyme, cooperativity of the active sites, and contributions of intersubunit interactions to any one active site.

The highly conserved tertiary structure of α-oxoamine synthases can allow for substantial plasticity, as demonstrated with circularly permuted murine erythroid ALAS variants [21,22]. Rearrangement of some secondary structural elements of ALAS does not prevent folding of the polypeptide chain into a structure compatible with binding of the PLP cofactor and assembly of the two subunits into a functional homodimer [21,22]. Simply linking the two ALAS monomers with a two amino acid spacer results in a monomeric enzyme (or “single chain dimer”) with distinct spectroscopic properties and substantially enhanced enzymatic activity compared to homodimeric ALAS [23]. Similarly, a naturally occurring marine viral “single chain dimeric” SPT has been discovered, and construction of yeast and mammalian SPT single-chain chimeras formed by linking the two highly similar, but structurally unique, LCB1 and LCB2 subunits resulted in functional enzymes, but with altered substrate specificities [24]. In addition, Han *et al.* [25] recently reported the finding of two small subunits of mammalian SPT (ssSPTa and ssSPTb), which can confer distinct acyl-CoA substrate specificities to the enzyme.

To investigate the unusual enhanced enzymatic activity resulting from linking ALAS dimers to form a monomer and help define the limits of structural plasticity in α-oxoamine synthases, we constructed and characterized “single chain dimeric” ALAS variants, in which one of the two active sites harbored a mutation eliminating measurable enzyme activity, and single-chain chimeras between WT or mutated ALAS and AONS. By combining two subunits into a single polypeptide chain, we altered one active site, while leaving the other intact, and hence assessed the role of each active site in the ALAS dimer. We report that the two active sites in ALAS/ALAS differentially contribute to the enhanced activity of the enzyme, even though the amount of ALA produced during the first turnover is identical in

both active sites. Further, the chimeric ALAS/AONS protein forms multi-functional dimers with both ALAS and AONS activities.

2. MATERIALS AND METHODS

2.1 Materials

All restriction enzymes, Vent DNA polymerase, and T4 DNA ligase were from New England Biolabs. Superdex 200 gel filtration resin was from Amersham Biosciences-GE Healthcare and DNA oligonucleotides were from Integrated DNA Technologies. Sodium dodecyl sulfate polyacrylamide gel electrophoresis reagents were acquired from Bio-Rad. All other reagents were purchased from Sigma-Aldrich Chemical Company or Fisher Scientific.

2.2 Methods

2.2.1 Construction of ALAS/ALAS and ALAS/AONS chimeric expression plasmids—Chimeras between murine, mature erythroid ALAS and *E. coli* AONS or between mutated forms of either ALAS or AONS and the WT enzymes were engineered using pGF23 [26] as the expression vector (Figure 1, Table 1). pTDT1, an expression plasmid for 6x-histidine-tagged *E. coli* AONS, was constructed by PCR-amplification of the *E. coli bioF* gene, which encodes the AONS protein, and subcloning of the PCR product into pGF23, such that the *bioF* gene replaced the ALAS-encoding fragment (see Supplementary Data).

The pTDT5 and pTDT4 expression plasmids (Table 1) were constructed to yield chimeric proteins between ALAS and AONS (Figure 1). Using the 5′ to 3′ convention for the "chimeric gene" under the control of the alkaline phosphatase promoter, pTDT5 contains the cDNA coding for ALAS linked to the following *bioF* gene for AONS through a *Mfe* I site, whereas in pTDT4, the *bioF* gene precedes the ALAS cDNA (Figure 1). These constructs were based on the pAC1 plasmid [21,22,23] (Figure 1), which contains two tandem ALAS cDNA sequences separated by an *Mfe*I cloning site.

The pTDT12 and pTDT17 expression plasmids (Table 1) were constructed using the pGF27 expression plasmid for the $ALAS^{K313A}$ variant [27] as the starting material for a DNA piece coding for the $ALAS^{K313A}$ mutation. The pGF27 plasmid was digested with *Kpn* I and *Xba* I, and the $ALAS^{K313A}$-encoding fragment was ligated into pTDT4 and pTDT5 digested with the same enzymes.

The pTDT8 plasmid (Table 1) was designed to encode a full-length ALAS with phenylalanine-341 mutated to alanine. To introduce the F341A encoding mutation into ALAS cDNA, the method previously described by Gong *et al.* was followed [28].

The pTDT14 and pTDT15 expression plasmids (Table 1) were constructed using pTDT8 as the source plasmid for the $ALAS^{F341A}$-encodingfragment. The pTDT8 plasmid was digested with *Kpn* I and *Xba* I, and the fragment containing the $ALAS^{F341A}$ mutation was isolated and subcloned into pTDT5 and pTDT4 to generate pTDT14 and pTDT15, respectively.

The pTDT7 expression plasmid encodes the ALAS/AONS chimera in which the AONS active-site lysine involved in the Schiff base linkage with the PLP cofactor, K236, is mutated to an alanine (Table 1; Figure 1). The method described by Gong *et al.* [28] was used to introduce the K236A-encoding mutation in the *bioF* gene harbored in pTDT5.

The pCA1 and pMG1 expression plasmids, encoding $ALAS^{K313A}$/ALAS and ALAS/$ALAS^{K313A}$, respectively, were constructed using the pAC1 and pGF27 plasmids (Table 1; Figure 1).

2.2.2 Biological screening for ALAS and AONS function—Competent *E. coli* HU227 and R872 cells were transformed by electroporation with expression plasmids containing the ALAS and AONS chimeric constructs. To screen for ALAS function, transformed HU227 cells were plated on Luria-Bertani medium (0.5% yeast extract, 1% tryptone, 1.0% NaCl and 1.5% agar) containing 50 μg/ml ampicillin. To screen for AONS function, transformed R872 cells were plated on M9 minimal medium containing 50 μg/ml ampicillin. M9 medium contains 1X M9-salts (12.8 g Na_2HPO_4-$7H_2O$, 3.0 g KH_2PO_4, 0.5g NaCl, and 1.0g NH_4Cl per 1 L), 2 mM $MgSO_4$, 0.1 mM $CaCl_2$, 0.4 % glucose, 0.1 % vitamin-free casamino acids and 1.5% agar.

2.2.3 Purification of ALAS, AONS, ALAS/ALAS, $ALAS^{K313A}$/ALAS, ALAS/$ALAS^{K313A}$ and ALAS/AONS—The purification of ALAS from *E. coli* DH5α cells harboring pGF23 was as previously described [26]. Recombinant *E. coli* AONS and chimeric ALAS/AONS were purified from *E. coli* DH5α cells harboring pTDT1 and pTDT5, respectively. Tandem ALAS variants (*i.e.*, ALAS/ALAS, $ALAS^{K313A}$/ALAS and ALAS/$ALAS^{K313A}$) were purified from *E. coli* strain BL21(DE3) overproducing cells harboring pAC1, pCA1 or pMG1. ALAS, AONS and the above tandem variants were expressed and purified following slight modifications to the purification described in [26]. Specifically, for both AONS and ALAS/AONS, the initial ammonium sulfate fractionation step was 20%. After stirring for 20 min at 4 °C, the solution was centrifuged at 27,000×g for 30 min at 4 °C, and the supernatant was further fractionated with ammonium sulfate to a final concentration of 40%.

For the purification of AONS, the protein pellet was resuspended in buffer A and loaded onto an Ultrogel ACA-44 gel filtration column equilibrated with buffer A. The protein solution was adjusted to 20% (w/v) ammonium sulfate and the subsequent chromatographic steps using Phenyl-Sepharose and Q-Sepharose anion exchange columns were as previously described [29].

The purification of ALAS/ALAS from bacterial cells harboring the pAC1 expression plasmid (Table 1) was according to a previously published method [21,22,23]. For the tandem ALAS variants, $ALAS^{K313A}$/ALAS and $ALAS^{K313A}$/ALAS encoded by pCA1 and pMG1, respectively (Table 1), the protein pellet was resuspended in buffer A and loaded onto a Superdex 200 column equilibrated with buffer A. The fractions containing protein were pooled and loaded onto a DEAE-sephacel resin equilibrated with buffer A. The resin was washed with buffer A, and the protein was eluted with buffer A containing 70 mM KCl. For the purification of ALAS/AONS, the protein pellet obtained after 40% ammonium sulfate fractionation was resuspended in buffer A, pH 7.9, and loaded onto an Ultrogel ACA-44 column equilibrated with the same buffer. The fractions containing protein were pooled and loaded onto a Q-Sepharose column equilibrated with buffer A, pH 7.9. The Q-Sepharose resin was washed with buffer A, pH 7.9, containing 25 mM KCl, until Abs_{280} of the “washed proteins” was lower than 0.1; ALAS/AONS was eluted from the Q-Sepharose resin with a 100 mM to 150 mM KCl gradient in buffer A, pH 7.5. The protein purity was assessed using SDS-PAGE. When the final product did not meet our purity criteria (*i.e.*, over 95% homogeneity as judged by SDS-PAGE), size exclusion chromatography with Sephadex 200 resin was used to eliminate protein contaminants. Protein-containing fractions were pooled and concentrated in an Amicon 8050 stirred cell with an YM30 membrane. The purified and concentrated enzyme (WT ALAS, AONS, ALAS/ALAS, $ALAS^{K313A}$/ALAS, ALAS/$ALAS^{K313A}$ or ALAS/AONS) was stored in liquid nitrogen.

Protein concentrations were determined with the bicinchoninic acid method using bovine serum albumin as the standard [30]. ALAS/AONS concentrations are reported on the basis of a subunit molecular mass of 96 kD, while ALAS/ALAS^{K313A} and ALAS^{K313A}/ALAS concentrations are reported on the basis of a subunit molecular mass of 112 kD.

2.2.4 Molecular mass determination by gel filtration chromatography—The native molecular mass of ALAS/AONS was determined using gel filtration chromatography as previously described by Cheltsov *et al.* [21].

2.2.5 Pimeloyl-CoA synthesis—Pimeloyl-CoA was synthesized as previously described by Ploux and Marquet [19]. Purity was assessed by reverse-phase HPLC and concentration was determined by measuring the absorbance at 260 nm and using an $\varepsilon^{260nm} = 16800\ M^{-1}\ cm^{-1}$.

2.2.6 Spectroscopic measurements—Absorption spectra were acquired at ambient temperature using a Shimadzu UV 2100 dual beam spectrophotometer, with a reference containing all components except the purified enzyme. Fluorescence spectra were collected on a Shimadzu RE-5301 PC spectrofluorophotometer using protein concentrations of 2–4 μM. Fluorescence blank spectra were collected from samples containing all components except enzyme immediately prior to the measurement of samples containing enzyme. The blank spectra were subtracted from the spectra of samples containing enzyme.

2.2.7 Steady-state kinetic characterization of ALAS/AONS, ALAS^{K313A}/ALAS, and ALAS/ALAS^{K313A}—ALAS steady-state activity of the ALAS/AONS chimera, ALAS^{K313A}/ALAS and ALAS/ALAS^{K313A} was determined at 30 °C using a continuous spectrophotometric assay as described previously for WT ALAS [31]. AONS steady-state activity of the of the ALAS/AONS chimera was determined at 30 °C using a coupled enzymatic spectrophotometric assay for AONS [32], which is similar to that developed for determination of ALAS activity [31]. Briefly, in the latter assay, α-ketoglutarate dehydrogenase was replaced by pyruvate dehydrogenase as the coupling enzyme, and the reactions contained 20 mM HEPES, pH 7.5, 3 mM $MgCl_2$, 1 mM pyruvic acid, 1 mM NAD^+ and 0.25 to 1 μM enzyme. Data were acquired using a Shimadzu UV 2100 dual-beam spectrophotometer. Enzymatic activity data were plotted *vs.* substrate concentration in which one of the substrate concentrations varied, while the second was kept constant. The steady-state kinetic parameters (*i.e.*, K_m^{Gly}, K_m^{SCoA}, and k_{cat} of the ALAS/AONS chimera, ALAS^{K313A}/ALAS and ALAS/ALAS^{K313A} and $K_m^{Alanine}$, K_m^{PCoA}, and k_{cat} of the ALAS/AONS chimera) were determined by fitting the data to the Michaelis-Menten equation using non-linear regression analysis software.

2.2.8 Rapid chemical quenched-flow experiments and data analysis—Rapid chemical quenched-flow experiments were performed using a SFM-400/Q mode quenched-flow apparatus (BioLogic Science Instruments, France), equipped with a circulating water bath to control the temperature of the reactants as described in Zhang and Ferreira [33]. ALA concentration in the quenched samples was also determined as previously described [33]. ALA produced at different reaction times were plotted against time and fitted to equation 1 [34], using the nonlinear least-squares regression analysis program SigmaPlot, where P_t represents the product concentration at an aging time t, A is the amplitude of the burst phase, k_b is the burst rate constant, k_{ss} is the steady-state rate constant, and E_0 is the total enzyme concentration [33].

$$P_t = A(1 - e^{-kbt}) + k_{ss}E_0t \quad \text{Equation 1}$$

3. RESULTS

3.1 *In vivo* activity screen of ALAS^{K313A}/ALAS and ALAS/ALAS^{K313A}

Positive genetic complementation of *hemA*$^-$ *E. coli* HU227 cells was utilized to assess the ALAS activity of ALAS^{K313A}/ALAS and ALAS/ALAS^{K313A}, which harbor the inactivating K313A mutation in either of the two linked ALAS subunits (Table 1 and Figure 1). HU227 cells can not produce ALA and only grow in a medium supplemented with ALA [35] or when transformed with a functional ALAS expression plasmid [18,36]. Indeed, while HU227 cells harboring the ALAS homodimer or the single chain dimeric ALAS/ALAS can grow in a medium without ALA [18,36], HU227 cells overproducing the K313A homodimer cannot [18] (Table 2). Both ALAS^{K313A}/ALAS and ALAS/ALAS^{K313A} variants retained function as indicated by the ability of transformed HU227 cells to grow when harboring either variant (Table 2).

3.2 Spectroscopic characterization of ALAS^{K313A}/ALAS and ALAS/ALAS^{K313A}

Although, as previously reported [23], the UV/visible absorbance spectra for both ALAS and the single chain dimeric ALAS/ALAS exhibited the characteristic maxima for PLP-dependent enzymes at ~330 and ~420 nm, the prominence of these absorbance bands varied between the spectra of the two proteins (Figure 2). At pH 7.5 the ratio of the 420 nm to 330 nm absorbance changed from 0.44 for ALAS to 0.67 for ALAS/ALAS (Figure 2). Similarly, the distinct absorbances at these wavelengths in the UV/visible spectra of the ALAS^{K313A}/ALAS and ALAS/ALAS^{K313A} variants resulted in a 420 to 330 nm absorption ratio of 0.35 and 0.58 at pH 7.5 for ALAS^{K313A}/ALAS and ALAS/ALAS^{K313A}, respectively (Figure 2). The ~330 and ~420 nm maxima were previously attributed to the substituted aldimine and ketoenamine forms of the internal aldimine between PLP and the ε-amino group of K313, respectively [23]. Clearly, the lysine mutations reveal that the cofactor internal aldimines differ between the two active sites in the linked enzymes.

3.3 Kinetic characterization of the ALAS^{K313A}/ALAS and ALAS/ALAS^{K313A} variants and determination of the dissociation constants for the binding of ALA

The steady-state kinetics of the ALAS^{K313A}/ALAS and the ALAS/ALAS^{K313A} reactions were examined, and the results are presented in Table 3. Previously, it was reported that linking the two ALAS subunits into the single chain dimeric ALAS/ALAS resulted in over 5-fold and 28-fold increases in the k_{cat} and k_{cat}/K_m^{SCoA} values, respectively [23]. To determine the individual contribution of the two active sites to the overall steady-state activity of ALAS/ALAS, the steady-state kinetic parameters of the ALAS^{K313A}/ALAS and ALAS/ALAS^{K313A} variants, in which the K313A mutation [27,37] was independently introduced in each of the two active sites, were determined (Table 3). While the K313A mutation in ALAS^{K313A}/ALAS decreased the k_{cat} 2.5-fold, the same mutation in ALAS/ALAS^{K313A} resulted in a 12.6-fold decrease of the k_{cat} value. Similarly, the catalytic efficiencies of ALAS^{K313A}/ALAS for glycine and succinyl-CoA were decreased approximately 2.9- and 1.8-fold, respectively, whereas those of ALAS/ALAS^{K313A} were reduced approximately 9- and 51-fold for glycine and succinyl-CoA, respectively. These findings suggest that linking the N-terminus of one subunit to the C- terminus of the other subunit in ALAS/ALAS may have created strain that slightly hindered the steady-state enzymatic activity of the N-terminal active site, while accentuating the activity of the C-terminal active site.

3.4 Pre-steady-state burst experiments for ALAS^{K313A}/ALAS and ALAS/ALAS^{K313A}

As with the ALAS-catalyzed reaction, the rate-limiting step for the single chain dimeric ALAS occurs after the chemical step and is proposed to be associated with a protein conformational change leading to ALA release [23]. To determine if the rate-limiting step of the reactions catalyzed by the K313A single chain dimeric variants occurs after the chemical step, we explored the events occurring at the active sites by performing rapid quenched-flow experiments and seeking a pre-steady-state burst of product formation in the ALAS^{K313A}/ALAS- and ALAS/ALAS^{K313A}-catalyzed reactions (Figure 3). The time courses for the reaction of either ALAS^{K313A}/ALAS or ALAS/ALAS^{K313A} were determined by mixing a solution containing glycine (400 mM)-saturated enzyme (30 μM) with succinyl-CoA (300 μM). At various times after mixing, the reaction was quenched by the addition of 0.14 M perchloric acid (final concentration) and the ALA concentration in the quenched reaction mixture was determined as described in [33]. The time-dependent formation of ALA is illustrated in Figure 3. The reaction of ALAS^{K313A}/ALAS occurred with a burst in ALA production at a rate of 30.6 ± 4.2 s^{-1}, whereasthe ALA formation burst of the ALAS/ALAS^{K313A} reaction was at a rate of 45.1 ± 6.1 s^{-1}. These burst rates are similar to the burst rate previously reported for the ALAS/ALAS reaction, 48.6 ± 6.1 s^{-1} [23]. Further, in both cases, the ALA burst was followed by a steady-state product accumulation at a significantly slower rate (<100-fold), corresponding to a rate-limiting step preceding subsequent turnover. We assigned this step to ALA release, presumably a protein conformational change leading to ALA release as postulated for the ALAS- and ALAS/ALAS-catalyzed reactions [33,38]. Another important piece of information provided by the burst experiments shown in Figure 3 relates to the burst amplitudes, representing the concentration of ALAS active sites for the reactions. The burst amplitudes were 0.25/active site and 0.21/active site for ALAS^{K313A}/ALAS and ALAS/ALAS^{K313A}, respectively, nearly 50% of the burst amplitude previously determined for ALAS/ALAS, 0.49/active site [23]. These results are consistent with the number of the active sites of either ALAS^{K313A}/ALAS or ALAS/ALAS^{K313A} being roughly 50% of that of ALAS/ALAS and also indicate that the different contributions of each of the two active sites of ALAS/ALAS to its steady-state activity emanate from a step occurring after ALAS chemistry.

3.5 Biological screening for ALAS and AONS function

The determination of the crystallographic structures of ALAS [8] and AONS [10] confirmed the prediction drawn from the high degree of sequence similarity between ALAS and AONS (37%) that these two α-oxoamine synthases have similar 3D fold and active site architecture. To extend our studies on the plasticity of the PLP-binding and active site of ALAS to other members of the α-oxoamine synthase family, chimeras of ALAS and AONS and chimeras of singly-mutated ALAS variants and AONS were constructed (Table 1 and Figure 1). The two major objectives were 1) to determine whether the chimeras retain ALAS and AONS activities and 2) to examine the active site arrangement in the ALAS/AONS chimera. Both ALAS/AONS and AONS/ALAS exhibited ALAS and AONS activities as assessed by the positive genetic complementation of *hemA*$^{-}$ HU227 and *bioF*$^{-}$ R872 cells, which are ALA/heme [35,39] and biotin auxotrophs [40], respectively (Table 2). From these *in vivo* activity assays, ALAS/AONS and AONS/ALAS appear to be bifunctional enzymes.

To start addressing the question related to the active site arrangement of ALAS/AONS chimera, directed-mutagenesis of critical residues in ALAS and AONS had to be established. K236 of *E. coli* AONS, the conserved active site lysine involved in PLP binding and catalysis [32], corresponds to K313 of murine ALAS [3,37]. Thus, when the K236A mutation was introduced in the AONS homodimer, *bioF*$^{-}$ R872 cells did not grow in a medium without biotin (data not shown), similar to the absence of growth of *hemA*$^{-}$ HU227 cells overproducing ALAS^{K313A} when plated onto a medium lacking ALA (Table 2). The

crystal structure of the *R. capsulatus* ALAS homodimer revealed that amino acids of the two polypeptide chains contribute to the same active site, which is located at the dimer interface [8]. For example, F276 (*R. capsulatus* ALAS numbering or F341 in the equivalent murine erythroid ALAS numbering), a phenylalanine crucial for interaction with the pantetheine moiety of CoA, and the lysine involved in the Schiff base linkage participate in the architecture of the same active site but reside in different polypeptide chains. Of significance to this study, F341 is critical to ALAS function, as the F341A mutation abolished the production of ALA necessary to sustain growth of HU227 cells on a selective medium (Table 2). Thus, while K313 and F341 are critical for function of the murine erythroid ALAS homodimer, of the corresponding K236 and Y264 [10], only K236 is essential for function in the *E. coli* AONS homodimer.

The three possible arrangements for the active sites of ALAS/AONS chimera are 1) formation of two active sites with the contribution of amino acids from one ALAS and one AONS polypeptide chains to each active site (Figure 4B) in an analogous arrangement to that of single chain dimeric ALAS/ALAS (Figure 4A); 2) formation of four active sites with the contribution of amino acids from one ALAS and one AONS polypeptide chains to each active site (Figure 4C); 3) formation of four active sites with two of the active sites being formed with only ALAS amino acids and the other two of the active sites with only AONS amino acids (Figure 4D), such that they represent WT ALAS- and AONS-like active sites. While the first active site arrangement would result from one single, chimeric polypeptide chain (Figure 4B), the latter two active site arrangements would arise from two chimeric polypeptide chains (Figures 4C and 4D). The determined molecular mass of ~182 KDa for the chimeric ALAS/AONS (see below and Figure 5) ruled against a single chain, dimeric ALAS/AONS and the active site arrangement depicted in Figure 4B. To distinguish between the other two possibilities for the active site arrangement of the ALAS/AONS chimera (Figures 4C and 4D), an experimental approach involving the use of specific amino acid mutations targeted to abolish either ALAS or AONS function and biological selection systems (*E. coli* HU227 and *E. coli* R872) was followed. If the active site arrangement in Figure 4C were correct the K313A mutation would eliminate ALAS function in two of the four active sites, and the AONS residues in one or two of the remaining sites would have to complement the ALAS residues, yielding a chimeric protein with ALAS and AONS activities. In contrast, with the active site arrangement presented in Figure 4D, the ALAS and AONS activities arise from WT ALAS- and AONS-like active sites, and thus a deleterious mutation of a critical active site residue in ALAS or AONS would produce a chimeric enzyme with impaired ALAS or AONS activity. HU227 cells transformed with either pTDT12 or pTDT17 [*i.e.*, expression plasmids for the ALAS/AONS chimera harboring the K313A mutation in ALAS (*i.e.*, Table 1)] did not support the growth of these cells in an ALA-depleted medium (Table 2). However, R872 cells harboring either of these two plasmids could grow in a medium without biotin. A similar situation was observed with the chimeras $ALAS^{F341A}$/AONS and AONS/$ALAS^{F341A}$, in which the phenylalanine at position 341 of murine erythroid ALAS was substituted with an alanine (Table 2). When the ALAS sequence was maintained intact and a mutation of the Schiff base linkage-lysine residue was introduced into AONS (*i.e.*, K236A), the generated chimeric proteins, $AONS^{K236A}$/ALAS or ALAS/$AONS^{K236A}$, could rescue the growth of HU227 cells in a medium without ALA but not of R872 cells in a non-biotin supplemented medium (Table 2). Taken together, these findings are consistent with the active site arrangement for ALAS/AONS depicted in Figure 4D, in which the active sites responsible for ALAS activity are built with ALAS residues, while those with AONS activity are made of AONS residues.

3.6 Oligomeric state of the ALAS/AONS chimera

Although ALAS/AONS and AONS/ALAS could be overproduced as active chimeric enzymes in *E. coli* DH5α cells (data not shown), only ALAS/AONS could be purified. Poor solubility and low stability were among the factors preventing the purification of AONS/ALAS.

The molecular mass of each subunit of the WT ALAS and WT AONS homodimers is ~56 and ~40 kD, respectively. Thus a single chimeric subunit, derived from the fusion of an ALAS and AONS polypeptide, was expected to be ~96 kD. This is in agreement with the molecular mass estimated by SDS-PAGE (Figure 5, inset). The molecular mass of the native ALAS/AONS chimera was determined to be ~182 kD (Figure 5), consistent of a "homodimer" of ~96 kD subunits. Further, coupled enzyme assays confirmed that the 182-kD protein exhibits both ALAS and AONS activities, indicating that the ALAS/AONS chimera is bifunctional as a homodimer of two ~96 kD chimeric polypeptide subunits.

3.7 Spectroscopic characterization of AONS and ALAS/AONS

At pH 7.5, absorbance maxima at ~330 and ~420 nm were observed in the ALAS/AONS chimera (Figure 6A). Because the UV-visible spectra of both ALAS and AONS exhibited maxima at 330 nm and 420 nm, their fluorescence spectra were examined for distinctive features among ALAS, AONS and ALAS/AONS. With excitation at 420 nm, the PLP cofactor of either ALAS or AONS exhibited a fluorescence emission maximum at 510 nm for ALAS and AONS (Figure 6B), albeit the magnitude of the 510 nm fluorescence emission maximum was more than three times greater for the AONS cofactor than that of ALAS. Similar to AONS and ALAS, the PLP cofactor of the ALAS/AONS chimera exhibited a fluorescence emission maximum at 510 nm upon excitation at 420 nm, and the magnitude of this fluorescence emission maximum fell between the values observed for the PLP cofactor of ALAS and AONS (Figure 6B). Upon excitation at 330 nm, the fluorescence emission spectra of ALAS and AONS exhibited maxima at 385 nm and 430 nm, respectively, while the fluorescence emission spectrum of the ALAS/AONS chimera displayed a broad emission band between 385 nm and 430 nm (Figure 6C).

3.8 Steady-state and transient kinetics of ALAS/AONS

To examine the ALAS and AONS activities of the ALAS/AONS chimera, the steady-state kinetic parameters of the chimeric protein associated with both activities were determined using substrates for ALAS and AONS (Tables 4 and 5). Regarding the ALAS activity, the k_{cat} decreased almost 40%, the catalytic efficiency for glycine increased ~1.4-fold, and the catalytic efficiency for succinyl-CoA remained virtually the same relative to ALAS (Table 4). With respect to the AONS activity, while the value for k_{cat} decreased approximately 50%, the catalytic efficiencies towards alanine and pimeloyl-CoA of the ALAS/AONS chimera were similar to those of AONS (Table 5).

Using chemical quenched-flow, pre-steady-state experiments of the ALAS reaction were performed under multi-turnover conditions, to examine the extent of ALA production by ALAS/AONS and ascertain the reactivity of the ALAS active sites in the ALAS/AONS chimera (Figure 7). The time course associated with ALA formation was biphasic, described by a rapid, exponential phase (*i.e.*, burst phase) followed by a slower linear phase (*i.e.*, steady-state phase). The first turnover occurred at a rate of $13.2 \pm 2.6\ s^{-1}$, while subsequent turnovers took place at a rate of $0.015\ s^{-1}$. The observed pre-steady state burst clearly indicated that the rate-limiting step in the overall ALAS reaction occurs after the chemical step, ALA formation, and corresponds to release of the product from the active site. While the values for the burst and the steady-state rates were approximately 70% and 50% of those previously determined for the wild-type ALAS-catalyzed reaction [33] the burst amplitude

of 0.10/active site was similar to that formerly observed with wild-type ALAS [33]. Significantly, the ~50% decrease in the value of the steady-state rate agrees with that inferred from the experiments performed under steady-state conditions (above). Thus, ALA is formed and accumulated similarly on the active sites of ALAS and ALAS/AONS, and the diminished steady-state ALAS activity of the ALAS/AONS chimera in relation to that of ALAS must arise from a step occurring after the reaction chemistry, presumably a strained protein conformational change associated with product release.

4. DISCUSSION

ALAS and other fold-type I PLP-dependent enzymes function as homodimers with two active sites per dimer; each active site is created at the interface between the two monomeric subunits [1,2]. The crystal structure of the *R. capsulatus* ALAS holoenzyme revealed that the enzyme symmetrically binds two PLP molecules, one at each active site [8]. Previously, we demonstrated that linking the two subunits of ALAS into a single polypeptide chain yielded a more-active enzyme that functioned as a single-chain dimer [23]. Although linking the N-terminus of one subunit and the C-terminus of the adjacent subunit without the introduction of a polypeptide linker did not affect the global conformation, changes in the environment of the PLP cofactor altered the predominant tautomeric form of the internal aldimine, which contributed to the greater activity of the single-chain dimer [23]. However, it was not clear if these changes affected the enzymatic activity of each active site to a similar extent. To determine whether the two active sites in ALAS/ALAS contribute equally to enzymatic activity, we characterized variants in which one of the two active sites had no measurable enzymatic activity due to a mutation of the conserved K313 residue that binds to the cofactor.

Spectral characterization of ALAS/ALAS^{K313A} and ALAS^{K313A}/ALAS revealed asymmetric cofactor environments in the two active sites, which was reflected in the disproportionate kinetic behavior of the two active sites. In contrast to ALAS/ALAS and ALAS^{K313A}/ALAS, in which the catalytic rates increased 5-fold and 2-fold, respectively, relative to the values for WT ALAS, the catalytic rate decreased approximately 50% for ALAS/ALAS^{K313A}. The concentration of catalytically active sites in ALAS/ALAS^{K313A} and ALAS^{K313A}/ALAS was half that of the ALAS/ALAS but, unlike the variations observed in the steady-state rates, the chemical rates were similar in all three forms. As with ALAS/ALAS and WT ALAS [23,33], the pre-steady-state burst kinetics results for the two K313A variants were consistent with the rate-limiting step occurring after the reaction chemistry.

In ALAS, the rate-limiting step has been ascribed to the opening of an active site loop that allows ALA release; the rate of this assigned loop opening closely corresponds to the steady-state rate [33,38,41]. Mutations introduced in the 18-amino acid active site loop yielded variants of ALAS with significantly increased rates of loop opening and product release [41]. Thus, the variations observed in the steady-state kinetic parameters of the single chain dimer are likely to be due to alterations in the energy barrier for the conformational change required for ALA release. The ALAS crystal structure indicates that the N-terminus of one subunit and the C-terminus of the adjacent subunit are located near the surface on opposite faces of the holoenzyme [8]. The strain resulting from linking the remote N- and C-termini of two ALAS subunits in ALAS/ALAS appears to increase the energy barrier for product release at one site while decreasing the barrier at the other; that is, the steady-state enzymatic activity is enhanced at one active site and hindered at the other. Consequently, the active sites contribute asymmetrically to enzyme function.

Generally, the active sites in fold type I PLP-dependent enzymes are equivalent and independent [2], although some examples of kinetic asymmetry have been documented. In glutamate-1-semialdehyde aminomutase (GSAM), allosteric interactions between active sites lead to inactivation of the site in one subunit by the activation of the site in the other subunit [42]. In aspartate aminotransferase (AAT), dissimilar lattice contact in the crystalline enzyme contributes to kinetic asymmetry in the active sites, although the active sites display kinetic equivalence in solution [43]. In addition, heterodimeric variants created for a number of complementation studies have contained asymmetric active sites [18,44,45,46], but the creation of ALAS/ALAS is the first example of engineered active site asymmetry without the introduction of active site mutations in fold-type I PLP-dependent enzymes. This linked dimer made it possible to alter and examine one active site in the presence of the other, which is a difficult undertaking with a “two-polypeptide chain dimer”.

We reasoned that the steady-state rates in the functioning active sites of either ALAS/ $ALAS^{K313A}$ or $ALAS^{K313A}$/ALAS would be 50% of that of the ALAS/ALAS single chain dimer, in which both sites contribute to enzyme function. Thus, the sum of the steady-state rates of ALAS/$ALAS^{K313A}$ and $ALAS^{K313A}$/ALAS would equal that of ALAS/ALAS. Clearly, this was not the case. The unequal steady-state rates of ALAS/$ALAS^{K313A}$ and $ALAS^{K313A}$/ALAS (~8% and ~40% of the steady-state rate of ALAS/ALAS, respectively) and the sum of their rates at about 50% of the steady-state rate of ALAS/ALAS led us to conclude that the two active sites do not contribute equally to the steady-state activity of the non-mutated single-chain dimer. Conversely, studies in the unlinked $ALAS^{K313A}$ and$ALAS^{R149A}$ heterodimer, containing one non-active site with both K313A and R149A mutations and one WT catalytically active site, show that the variant heterodimer retained approximately 50% of the activity observed in the ALAS homodimer [18]; that is, the WT active site was not significantly affected by mutations at the adjacent site, and the two sites appeared to work independently in the ALAS homodimer. Thus, linking the termini of the two ALAS subunits made the two active sites to function asymmetrically by likely altering the intermolecular dynamics such that movement of the active site loop for product release was greatly enhanced at one active site and impaired at the other.

Because the single-chain ALAS dimer showed structural plasticity and had increased activity, we wondered whether the structural plasticity would extend to single-chain chimeras constructed from two members of the α-oxoamine synthase family, ALAS and AONS. We also hypothesized that it might be possible to generate an enzyme with novel activity by creating hybrid ALAS/AONS active sites. *In vivo* assays indicated that the ALAS/AONS and AONS/ALAS chimeras possessed both ALAS and AONS activities. Thus, the chimeric protein had sufficient structural plasticity to achieve the conformations necessary to produce both enzymatic activities. The linking of two ALAS subunits did not significantly affect the dimeric interface or the folding of the core in the individual subunits, and the dissociation of the dimeric interface of ALAS and the ALAS/ALAS single-chain dimer exhibited similar free energies and resulted in stable intermediates that retained a substantial amount of their secondary and tertiary structure [21,22]. Similarly, we would not expect the linking of ALAS and AONS to strongly affect the folding core or subunit interface of the two domains, and it is not surprising that the two domains retained their overall structural character given that the entire ALAS and AONS polypeptides were used in the creation of the chimeras.

Despite our initial hypothesis that the chimeric protein would create chimeric active sites with potentially novel enzymatic activities, both ALAS/AONS and AONS/ALAS appeared to function as chimeric homodimers with functionally independent ALAS and AONS modules. In these modules, two active sites exhibiting ALAS activity were built exclusively with ALAS residues, and two active sites with AONS activity were built with AONS

residues (Figure 4D). The chimeric proteins seem to assemble forming wild-type active sites. The implication is that other interactions besides those at the active site contribute to the recognition for the dimer interface, and those recognition elements are specific for a particular enzyme. Nonetheless, the dimerization of two chimeric polypeptides into a bifunctional homodimer with functionally independent ALAS and AONS modules suggests that the structural plasticity observed in ALAS can be extended to other members of the α-oxoamine synthase family. It is possible that creating a chimera from individual domains of each protein (for example, the N-terminal domain of ALAS and the catalytic and C-terminal domains of AONS) would produce a functional hybrid, but this remains to be tested.

Although we succeeded in expressing both the ALAS/AONS and AONS/ALAS chimeras as active enzymes, we were only able to purify the ALAS/AONS chimera. The molecular mass of the native ALAS/AONS chimera was consistent with that of a homodimer containing two chimeric polypeptide subunits. The fluorescence spectra exhibited by the ALAS/AONS chimera were distinct from those of ALAS and AONS and were consistent with an enzyme exhibiting a mixture of ALAS and AONS spectroscopic characteristics. The ALAS and AONS steady-state kinetic activities were diminished by roughly one-half in the chimera, and the catalytic efficiencies were not impaired. The pre-steady-state kinetic analysis for the ALAS reaction demonstrated that ALA formation in the ALAS sites of ALAS/AONS was similar to that in ALAS, with the rate-limiting step occurring after chemical catalysis.

The linking of two proteins or functional domains in natural and *de novo* fusion proteins generally involves a peptide linker [47,48,49]. A primary goal of linker engineering is to effectively separate the two functional domains to avoid intermolecular strain and prevent unwanted interactions between the two modules [47,48,50,51,52]. Because our objective was to facilitate interaction between the subunits of ALAS/ALAS and the AONS and ALAS chimeras, only two amino acids (Glu-Leu), which were introduced with the construction of a restriction site between the cDNAs, link the two subunits. Like both ALAS single-chain dimeric variants, the linking of the ALAS and AONS subunits appeared to change the energy barrier associated with the structural rearrangement that occurs upon ALA formation to allow product release. It is likely that the use of the short dipeptide to link the ALAS C-terminus with the N-terminus of either ALAS or AONS introduced intermolecular strain which altered conformational flexibility.

Remarkably, the strain introduced with the short linker did not significantly impair the catalytic efficiencies in any of the fusion proteins. In fact, the catalytic efficiency for succinyl-CoA increased roughly 15- and 30-fold in $ALAS^{K313A}$/ALAS and ALAS/ALAS, respectively (Table 3). The short linker also appears to have altered the intermolecular dynamics and caused different extent of the active site loop motion at the two sites. While the loop motion and product release were greatly facilitated at one site, they were hindered at the other. However, since the degree of enhancement at one site was greater than the degree of hindrance at the other site, the resulting linked chain dimer (ALAS/ALAS) possessed greater enzyme activity than the “natural” wild-type homodimer (ALAS). Generally, efforts are made to avoid the introduction of strain when engineering hybrid proteins; however, with the increased use of high-throughput protein engineering, the introduction of intermolecular strain through linker domains may be a reasonable approach to creating new proteins with enhanced or novel functions. This might be particularly important if one takes into account that recruitment of domains and subunits, with alteration of domain architecture and oligomeric state, seems to represent one mechanism of how proteins evolve to acquire distinct functions with a limited number of scaffolds [43]. Oligomerization and domain fusion appeared to be a strategy adopted by transferases to shield hydrophilic ligands, contrasting to their homologous, and perhaps parent, hydrolases, in which the ligand molecules are exposed to water [43].

In summary, we constructed a dimeric enzyme from a single polypeptide chain such that each active site could be studied independently. We have shown that the two active sites in the ALAS/ALAS single-chain dimer make asymmetrical steady-state contributions to the activity of the enzyme. This and the reduced steady-state activity of the single-chain chimeras of ALAS and AONS relative to the parent enzymes are likely to be caused by differences in conformational changes at product release, which in turn are due to the strain introduced by joining the two subunits without a linker region. Although the chimeric ALAS/AONS and AONS/ALAS proteins did not form hybrid active sites, they were able to form dimers with separate regions of ALAS and AONS activity. Thus, the extensive structural plasticity seen in ALAS extends to another member of the α-oxoamine family, AONS, and other interactions in addition to those at the active site contribute to the recognition for the dimer interface of a specific enzyme.

Supplementary Material

Refer to Web version on PubMed Central for supplementary material.

Acknowledgments

We thank Dr. Dominic Campopiano (University of Edinburgh) for providing the *Escherichia coli* R872 strain and pET6HAONS and Dr. Charlotte S. Russell (City University of New York) for the *E. coli* HU227 strain. We also thank Ms. Michelle Grigsby for her technical assistance in the construction of some of the expression plasmids and purification of some batches of ALAS/ALAS.

FUNDING

This work was supported by the National Institutes of Health, U.S.A. (grants # DK63191 and #GM080270 to GCF).

Abbreviations used

ALAS	5-aminolevulinate synthase
ALA	5-aminolevulinate
AONS	8-amino-7-oxononanoate synthase
AON	8-amino-7-oxononanoate
AMPSO	3-([1,1-dimethyl-2-hydroxyethyl]amino)-2-hydroxypropane sulfonic acid
CD	circular dichroism
CoA	coenzyme A
DEAE	diethylaminoethyl
HEPES	N-(2-hydroxyethyl) piperazine-N′-(2-ethane sulfonic acid)
HPLC	high performance liquid chromatography
MOPS	4-morpholinepropanesulfonic acid
NAD^+	β-nicotinamide adenine dinucleotide
PCR	polymerase chain reaction
PLP	pyridoxal 5′-phosphate
PCoA	pimeloyl-coenzyme A
SDS-PAGE	sodium dodecyl sulfate polyacrylamide gel electrophoresis
SPT	serine palmitoyltransferase

SCoA	succinyl-coenzyme A
WT	wild-type

References

1. Christen P, Mehta PK. From cofactor to enzymes. The molecular evolution of pyridoxal-5′-phosphate-dependent enzymes. Chem Rec. 2001; 1:436–447. [PubMed: 11933250]
2. Eliot AC, Kirsch JF. Pyridoxal phosphate enzymes: mechanistic, structural, and evolutionary considerations. Annu Rev Biochem. 2004; 73:383–415. [PubMed: 15189147]
3. Ferreira GC, Gong J. 5-Aminolevulinate synthase and the first step of heme biosynthesis. J Bioenerg Biomembr. 1995; 27:151–159. [PubMed: 7592562]
4. Hunter GA, Ferreira GC. Molecular enzymology of 5-Aminolevulinate synthase, the gatekeeper of heme biosynthesis. Biochimica et Biophysica Acta (BBA) -Proteins & Proteomics. 2011 In Press, Corrected Proof.
5. Layer G, Reichelt J, Jahn D, Heinz DW. Structure and function of enzymes in heme biosynthesis. Protein Science. 2010; 19:1137–1161. [PubMed: 20506125]
6. Schneider G, Kack H, Lindqvist Y. The manifold of vitamin B6 dependent enzymes. Structure. 2000; 8:R1–R6. [PubMed: 10673430]
7. Yard BA, Carter LG, Johnson KA, Overton IM, Dorward M, Liu H, McMahon SA, Oke M, Puech D, Barton GJ, Naismith JH, Campopiano DJ. The structure of serine palmitoyltransferase; gateway to sphingolipid biosynthesis. J Mol Biol. 2007; 370:870–886. [PubMed: 17559874]
8. Astner I, Schulze JO, van den Heuvel J, Jahn D, Schubert WD, Heinz DW. Crystal structure of 5-aminolevulinate synthase, the first enzyme of heme biosynthesis, and its link to XLSA in humans. Embo J. 2005; 24:3166–3177. [PubMed: 16121195]
9. Schmidt A, Sivaraman J, Li Y, Larocque R, Barbosa JA, Smith C, Matte A, Schrag JD, Cygler M. Three-dimensional structure of 2-amino-3-ketobutyrate CoA ligase from *Escherichia coli* complexed with a PLP-substrate intermediate: inferred reaction mechanism. Biochemistry. 2001; 40:5151–5160. [PubMed: 11318637]
10. Alexeev D, Alexeeva M, Baxter RL, Campopiano DJ, Webster SP, Sawyer L. The crystal structure of 8-amino-7-oxononanoate synthase: a bacterial PLP-dependent, acyl-CoA-condensing enzyme. J Mol Biol. 1998; 284:401–419. [PubMed: 9813126]
11. Raman MCC, Johnson KA, Yard BA, Lowther J, Carter LG, Naismith JH, Campopiano DJ. The External Aldimine Form of Serine Palmitoyltransferase. J Biol Chem. 2009; 284:17328–17339. [PubMed: 19376777]
12. Ikushiro H, Fujii S, Shiraiwa Y, Hayashi H. Acceleration of the Substrate CÎ± Deprotonation by an Analogue of the Second Substrate Palmitoyl-CoA in Serine Palmitoyltransferase. J Biol Chem. 2008; 283:7542–7553. [PubMed: 18167344]
13. Ikushiro H, Islam MM, Okamoto A, Hoseki J, Murakawa T, Fujii S, Miyahara I, Hayashi H. Structural Insights into the Enzymatic Mechanism of Serine Palmitoyltransferase from *Sphingobacterium multivorum*. J Biochem (Tokyo). 2009; 146:549–562. [PubMed: 19564159]
14. Jahan N, Potter JA, Sheikh MA, Botting CH, Shirran SL, Westwood NJ, Taylor GL. Insights into the Biosynthesis of the Vibrio cholerae Major Autoinducer CAI-1 from the Crystal Structure of the PLP-Dependent Enzyme CqsA. J Mol Biol. 2009; 392:763–773. [PubMed: 19631226]
15. Spirig T, Tiaden A, Kiefer P, Buchrieser C, Vorholt JA, Hilbi H. The *Legionella* Autoinducer Synthase LqsA Produces an α-Hydroxyketone Signaling Molecule. J Biol Chem. 2008; 283:18113–18123. [PubMed: 18411263]
16. Tiaden A, Spirig T, Carranza P, Bruggemann H, Riedel K, Eberl L, Buchrieser C, Hilbi H. Synergistic Contribution of the Legionella pneumophila lqs Genes to Pathogen-Host Interactions. J Bacteriol. 2008; 190:7532–7547. [PubMed: 18805977]
17. Tiaden A, Spirig T, Hilbi H. Bacterial gene regulation by [alpha]-hydroxyketone signaling. Trends in Microbiology. 2010 In Press, Corrected Proof.

18. Tan D, Ferreira GC. Active site of 5-aminolevulinate synthase resides at the subunit interface. Evidence from in vivo heterodimer formation. Biochemistry. 1996; 35:8934–8941. [PubMed: 8688429]
19. Ploux O, Marquet A. The 8-amino-7-oxopelargonate synthase from *Bacillus sphaericus*. Purification and preliminary characterization of the cloned enzyme overproduced in Escherichia coli. Biochem J. 1992; 283(Pt 2):327–331. [PubMed: 1575677]
20. Ferreira GC, Neame PJ, Dailey HA. Heme biosynthesis in mammalian systems: evidence of a Schiff base linkage between the pyridoxal 5′-phosphate cofactor and a lysine residue in 5-aminolevulinate synthase. Protein Sci. 1993; 2:1959–1965. [PubMed: 8268805]
21. Cheltsov AV, Barber MJ, Ferreira GC. Circular permutation of 5-aminolevulinate synthase. Mapping the polypeptide chain to its function. J Biol Chem. 2001; 276:19141–19149. [PubMed: 11279050]
22. Cheltsov AV, Guida WC, Ferreira GC. Circular permutation of 5-aminolevulinate synthase: effect on folding, conformational stability, and structure. J Biol Chem. 2003; 278:27945–27955. [PubMed: 12736261]
23. Zhang J, Cheltsov AV, Ferreira GC. Conversion of 5-aminolevulinate synthase into a more active enzyme by linking the two subunits: spectroscopic and kinetic properties. Protein Sci. 2005; 14:1190–1200. [PubMed: 15840827]
24. Han G, Gable K, Yan L, Allen MJ, Wilson WH, Moitra P, Harmon JM, Dunn TM. Expression of a novel marine viral single-chain serine palmitoyltransferase and construction of yeast and mammalian single-chain chimera. J Biol Chem. 2006; 281:39935–39942. [PubMed: 17090526]
25. Han G, Gupta SD, Gable K, Niranjanakumari S, Moitra P, Eichler F, Brown RH, Harmon JM, Dunn TM. Identification of small subunits of mammalian serine palmitoyltransferase that confer distinct acyl-CoA substrate specificities. Proc Natl Acad Sci USA. 2009; 106:8186–8191. [PubMed: 19416851]
26. Ferreira GC, Dailey HA. Expression of mammalian 5-aminolevulinate synthase in *Escherichia coli*. Overproduction, purification, and characterization. J Biol Chem. 1993; 268:584–590. [PubMed: 8416963]
27. Ferreira GC, Vajapey U, Hafez O, Hunter GA, Barber MJ. Aminolevulinate synthase: lysine 313 is not essential for binding the pyridoxal phosphate cofactor but is essential for catalysis. Protein Sci. 1995; 4:1001–1006. [PubMed: 7663334]
28. Gong J, Hunter GA, Ferreira GC. Aspartate-279 in aminolevulinate synthase affects enzyme catalysis through enhancing the function of the pyridoxal 5′-phosphate cofactor. Biochemistry. 1998; 37:3509–3517. [PubMed: 9521672]
29. Webster SP, Alexeev D, Campopiano DJ, Watt RM, Alexeeva M, Sawyer L, Baxter RL. Mechanism of 8-amino-7-oxononanoate synthase: spectroscopic, kinetic, and crystallographic studies. Biochemistry. 2000; 39:516–528. [PubMed: 10642176]
30. Smith PK, Krohn RI, Hermanson GT, Mallia AK, Gartner FH, Provenzano MD, Fujimoto EK, Goeke NM, Olson BJ, Klenk DC. Measurement of protein using bicinchoninic acid. Anal Biochem. 1985; 150:76–85. [PubMed: 3843705]
31. Hunter GA, Ferreira GC. A continuous spectrophotometric assay for 5-aminolevulinate synthase that utilizes substrate cycling. Anal Biochem. 1995; 226:221–224. [PubMed: 7793621]
32. Webster SP, Campopiano DJ, Alexeev D, Alexeeva M, Watt RM, Sawyer L, Baxter RL. Characterisation of 8-amino-7-oxononanoate synthase: a bacterial PLP-dependent, acyl CoA condensing enzyme. Biochem Soc Trans. 1998; 26:S268. [PubMed: 9765987]
33. Zhang J, Ferreira GC. Transient state kinetic investigation of 5-aminolevulinate synthase reaction mechanism. J Biol Chem. 2002; 277:44660–44669. [PubMed: 12191993]
34. Johnson KA. Transient-State Kinetic Analysis of Enzyme Reaction Pathways. The Enzymes. 1992; XX:1–61.
35. Li JM, Brathwaite O, Cosloy SD, Russell CS. 5-Aminolevulinic acid synthesis in *Escherichia coli*. J Bacteriol. 1989; 171:2547–2552. [PubMed: 2651407]
36. Gong J, Ferreira GC. Aminolevulinate synthase: functionally important residues at a glycine loop, a putative pyridoxal phosphate cofactor-binding site. Biochemistry. 1995; 34:1678–1685. [PubMed: 7849027]

37. Hunter GA, Ferreira GC. Lysine-313 of 5-Aminolevulinate Synthase Acts as a General Base during Formation of the Quinonoid Reaction Intermediates. Biochemistry. 1999; 38:12526–12531. [PubMed: 10493823]
38. Hunter GA, Zhang J, Ferreira GC. Transient kinetic studies support refinements to the chemical and kinetic mechanisms of aminolevulinate synthase. J Biol Chem. 2007; 282:23025–23035. [PubMed: 17485466]
39. Sasarman A, Surdeanu M, Horodniceanu T. Locus determining the synthesis of delta-aminolevulinic acid in *Escherichia coli* K-12. J Bacteriol. 1968; 96:1882–1884. [PubMed: 4882033]
40. Del Campillo-Campbell A, Kayajanian G, Campbell A, Adhya S. Biotin-requiring mutants of *Escherichia coli* K-12. J Bacteriol. 1967; 94:2065–2066. [PubMed: 4864413]
41. Lendrihas T, Hunter GA, Ferreira GC. Targeting the Active Site Gate to Yield Hyperactive Variants of 5-Aminolevulinate Synthase. J Biol Chem. 2010; 285:13704–13711. [PubMed: 20194506]
42. Stetefeld J, Jenny M, Burkhard P. Intersubunit signaling in glutamate-1-semialdehyde-aminomutase. Proc Natl Acad Sci U S A. 2006; 103:13688–13693. [PubMed: 16954186]
43. Kirsten H, Gehring H, Christen P. Crystalline aspartate aminotransferase: lattice-induced functional asymmetry of the two subunits. Proc Natl Acad Sci U S A. 1983; 80:1807–1810. [PubMed: 6572940]
44. Onuffer JJ, Kirsch JF. Characterization of the apparent negative co-operativity induced in *Escherichia coli* aspartate aminotransferase by the replacement of Asp222 with alanine. Evidence for an extremely slow conformational change. Protein Eng. 1994; 7:413–424. [PubMed: 8177890]
45. Tan D, Harrison T, Hunter GA, Ferreira GC. Role of arginine 439 in substrate binding of 5-aminolevulinate synthase. Biochemistry. 1998; 37:1478–1484. [PubMed: 9484217]
46. Tarun AS, Theologis A. Complementation analysis of mutants of 1-aminocyclopropane- 1-carboxylate synthase reveals the enzyme is a dimer with shared active sites. J Biol Chem. 1998; 273:12509–12514. [PubMed: 9575209]
47. Wriggers W, Chakravarty S, Jennings PA. Control of protein functional dynamics by peptide linkers. Biopolymers. 2005; 80:736–746. [PubMed: 15880774]
48. Arai R, Ueda H, Kitayama A, Kamiya N, Nagamune T. Design of the linkers which effectively separate domains of a bifunctional fusion protein. Protein Eng. 2001; 14:529–532. [PubMed: 11579220]
49. Gokhale RS, Khosla C. Role of linkers in communication between protein modules. Curr Opin Chem Biol. 2000; 4:22–27. [PubMed: 10679375]
50. Carlsson H, Ljung S, Bulow L. Physical and kinetic effects on induction of various linker regions in beta-galactosidase/galactose dehydrogenase fusion enzymes. Biochim Biophys Acta. 1996; 1293:154–160. [PubMed: 8652621]
51. Seo HS, Koo YJ, Lim JY, Song JT, Kim CH, Kim JK, Lee JS, Choi YD. Characterization of a bifunctional enzyme fusion of trehalose-6-phosphate synthetase and trehalose-6-phosphate phosphatase of *Escherichia coli*. Appl Environ Microbiol. 2000; 66:2484–2490. [PubMed: 10831428]
52. Arai R, Wriggers W, Nishikawa Y, Nagamune T, Fujisawa T. Conformations of variably linked chimeric proteins evaluated by synchrotron X-ray small-angle scattering. Proteins. 2004; 57:829–838. [PubMed: 15390267]

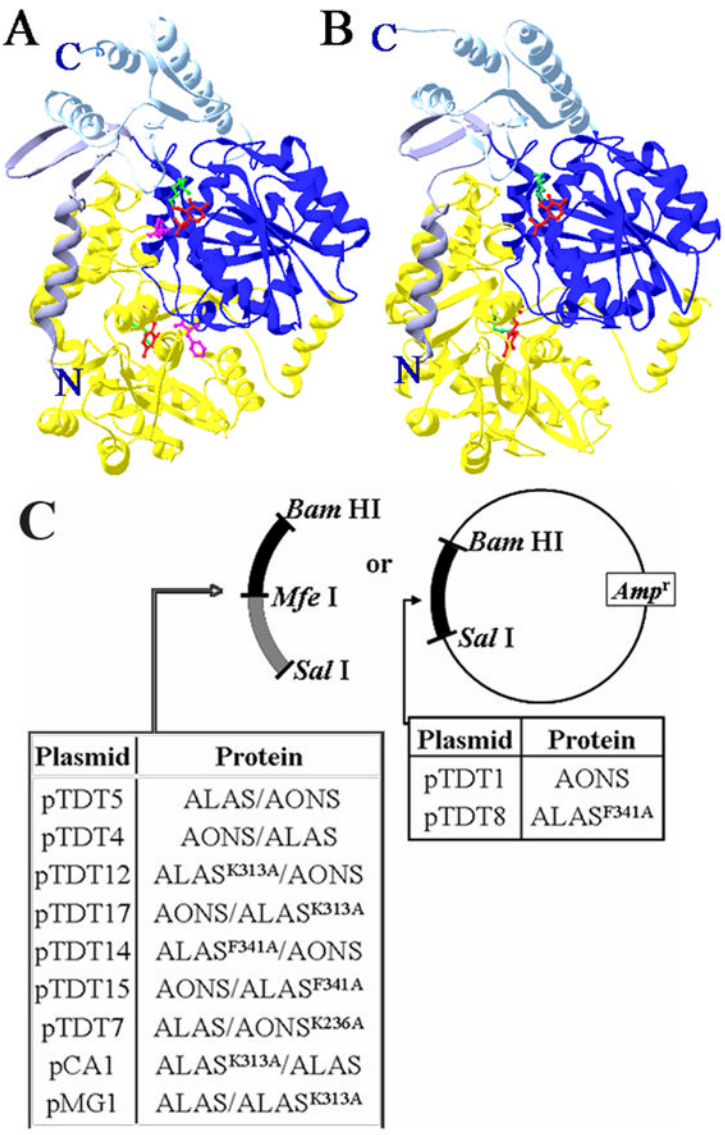

Plasmid	Protein
pTDT5	ALAS/AONS
pTDT4	AONS/ALAS
pTDT12	ALAS^{K313A}/AONS
pTDT17	AONS/ALAS^{K313A}
pTDT14	ALAS^{F341A}/AONS
pTDT15	AONS/ALAS^{F341A}
pTDT7	ALAS/AONS^{K236A}
pCA1	ALAS^{K313A}/ALAS
pMG1	ALAS/ALAS^{K313A}

Plasmid	Protein
pTDT1	AONS
pTDT8	ALAS^{F341A}

Figure 1. ALAS and AONS dimmers

(A–B) ALAS and AONS homodimers in ribbon representation with one subunit shown in yellow and the central catalytic core, N-terminal domain, and C-terminal domain of the second subunit rendered in dark, medium and light blue, respectively. **(A)** ALAS homodimer from *R. capsulatus* (PDB code: 2BWN). The PLP cofactor (*red*), the active site lysine (*green*) involved in the Schiff base linkage with PLP (K248 in *R. capsulatus* ALAS and K313 in murine erythroid ALAS) and F276 (*purple*; F341 in murine erythroid ALAS) are depicted in ball-and-stick representation. **(B)** AONS homodimer from *E. coli* (PDB code: 1BS0). The PLP cofactor (*red*) and the active site lysine (*green)* involved in the Schiff base linkage with PLP (K236) are depicted in ball-and-stick representation. **(C)** Schematic representation of the expression plasmids for mutated ALAS, AONS, ALAS/ALAS variants, and single-chain chimeras between ALAS (WT or mutated) and AONS (WT or mutated). Each of the expression plasmids contains a DNA fragment, encoding either a single protein subunit or a chimeric protein, under the control of the *phoA* promoter [26] and possesses an ampicillin resistance selectable marker. (See “Materials and Methods” for details). *Amp*^{r}, ampicillin resistance gene; *Bam* HI, *Mfe* I and *Sal* I, cloning sites.

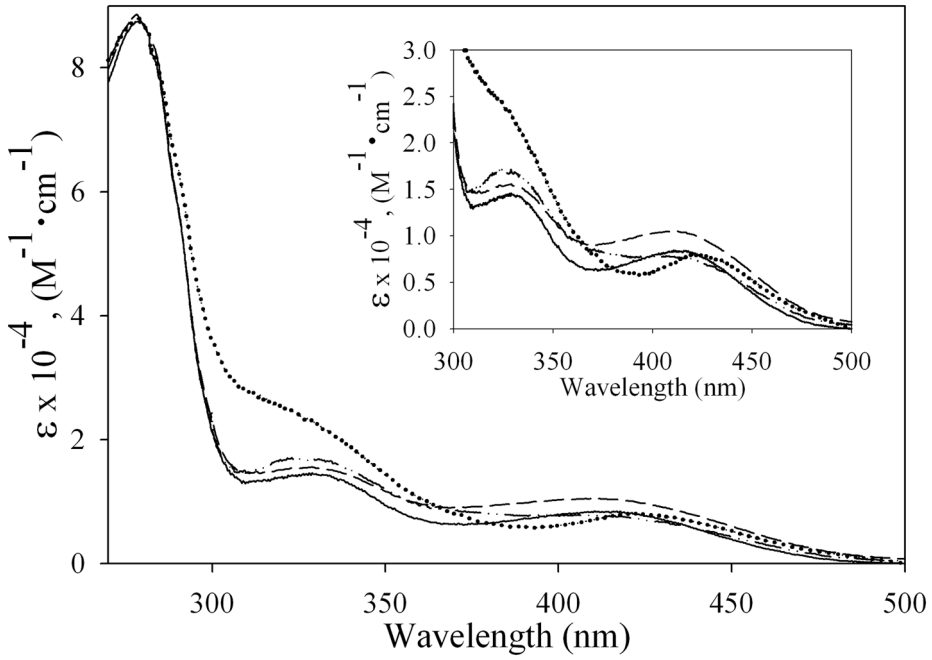

Figure 2. Absorption spectra of ALAS, ALAS/ALAS, ALAS^{K313A}/ALAS and ALAS/ALAS^{K313A}

The inset includes the region from 300–500 nm. Protein concentrations were adjusted to 7.75μM for ALAS/ALAS, 4.25μM for ALAS^{K313A}/ALAS and ALAS/ALAS^{K313A} or 10 μM for ALAS in 20 mM Hepes, pH 7.5. ALAS/ALAS^{K313A} (—), ALAS^{K313A}/ALAS (•••), ALAS/ALAS (--), and ALAS (– · · –).

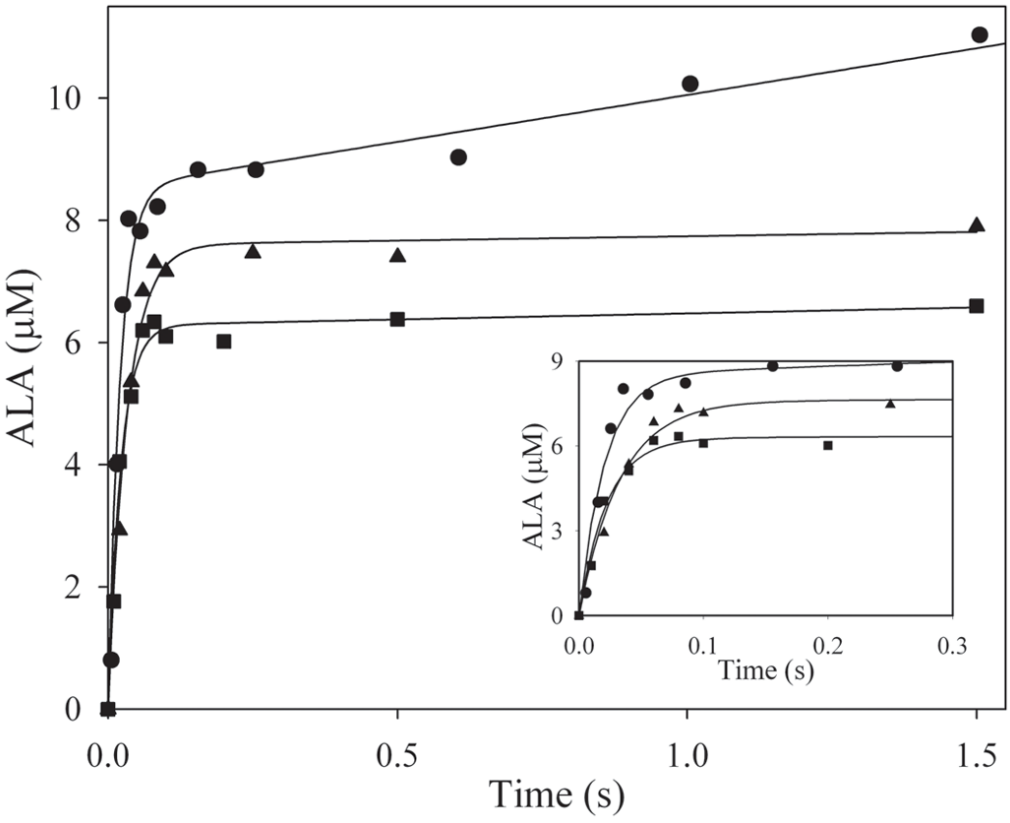

Figure 3. Kinetics of a pre-steady-state burst of ALA product in the ALAS/ALAS^{K313A} and ALAS^{K313A}/ALAS reactions

ALAS/ALAS^{K313A} (square) or ALAS^{K313A}/ALAS (triangle) (15 μM) preincubated with glycine (200 mM) was quickly reacted with succinyl-CoA (150 μM) at 20°C. The concentrations shown in *parentheses* are final concentrations after mixing. The *inset* illustrates the first 0.3 seconds of the reaction time course. The curves represent the best fits to equation 1. For comparison, the time course for the reaction of ALAS/ALAS (8.6 μM) (filled circles) under the experimental conditions described above is included [23].

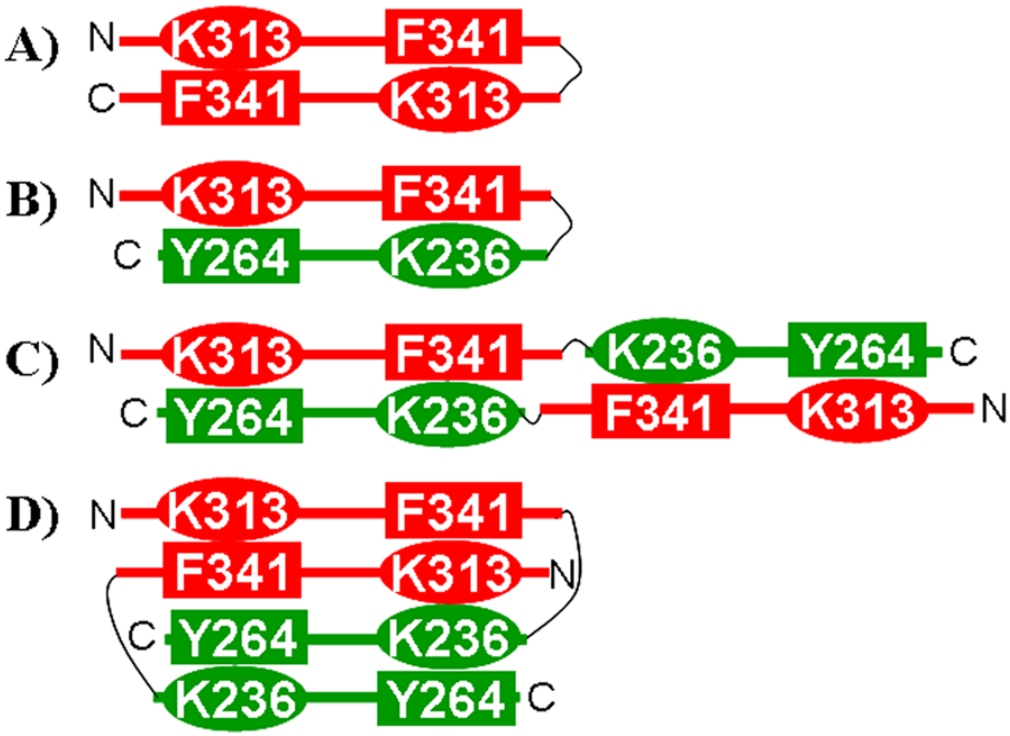

Figure 4. Schematic representation illustrating the active site arrangement for ALAS/ALAS and possible active site arrangements for ALAS/AONS

Red bars represent ALAS polypeptide chains, with the essential active site residues K313 and F341 from one single polypeptide chain contributing to separate active sites. Green bars represent AONS polypeptide chains, with the essential active site residues K236 and Y264 from one single polypeptide chain contributing to separate active sites. In (A) and (B), there are two active sites per single chain dimer, whereas in (C) and (D), there are four active sites per chimeric ALAS/AONS dimer. (A) Active site arrangement of the ALAS/ALAS "single chain dimer". (B) – (D) Possible active site arrangements for ALAS/AONS. (B) ALAS/AONS single chain dimer. (C) ALAS/AONS chimeric dimer with "hybrid" active sites comprised of both ALAS and AONS residues. (D) ALAS/AONS chimeric dimer with two of the active sites containing only ALAS residues and the other two active sites containing only AONS residues.

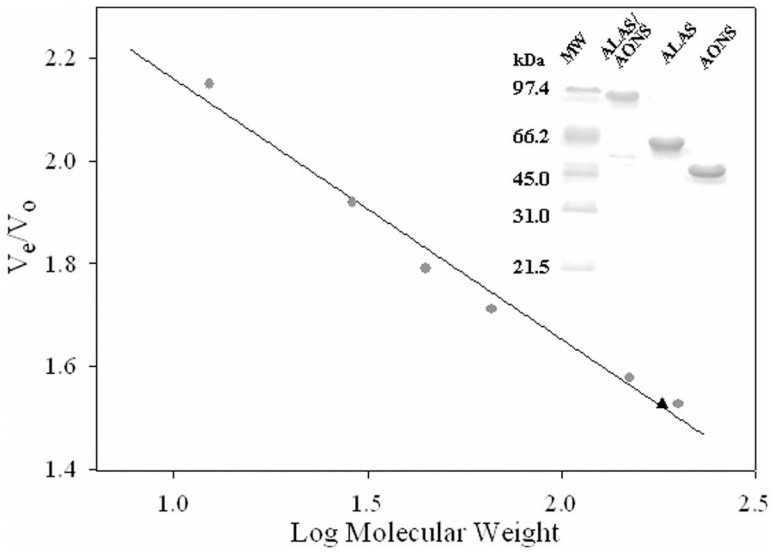

Figure 5. Determination of the molecular mass of the ALAS/AONS chimera by gel filtration chromatography

ALAS/AONS (5 mg) was applied to a Pharmacia Sephadex 200 filtration column and eluted as previously described [21]. The molecular mass calibration curve for the Superdex 200 column used cytochrome *c* (12.4 kDa), carbonic anhydrase (29.0 kDa), ovalbumin (45 kDa), bovine serum albumin (66.0 kDa), alcohol dehydrogenase (150.0 kDa), and β-amylase (200.0 kDa) as protein standards (indicated by circles). The ALAS/AONS chimera is indicated by a triangle. (*Inset*) 12.5% SDS-PAGE of the purified ALAS, AONS and ALAS/AONS chimera, which were detected using Coomassie Brilliant Blue staining. Approximately 5 μg of each protein sample was loaded per lane.

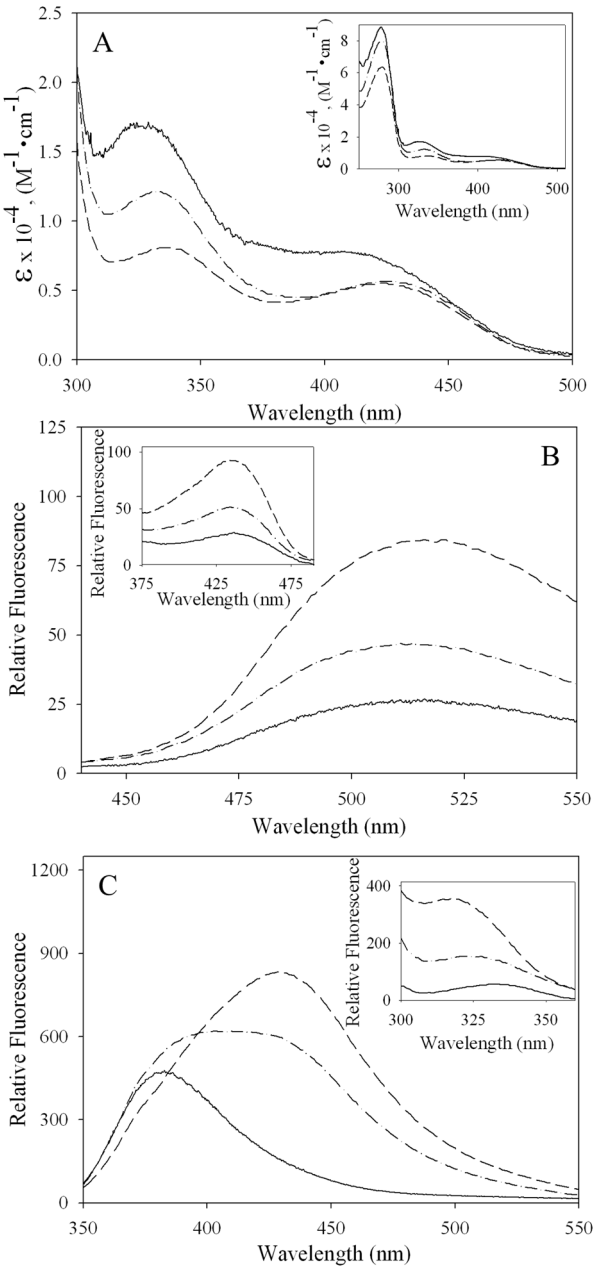

Figure 6. Absorption and fluorescence spectra of ALAS, AONS and ALAS/AONS. (A) UV-visible absorption spectra

The inset includes the region from 300–510 nm. Fluorescence emission spectra upon excitation at (B) 420 nm and (C) 330 nm and fluorescence excitation spectra upon emission at 510 nm (*inset B*) and 385 nm (*inset C*). For absorption spectra, protein concentrations were adjusted to 15 μM (AONS and ALAS) or 7.5 μM (ALAS/AONS) and for fluorescence spectra, protein concentrations were adjusted to 4 μM (AONS and ALAS) or 2 μM (ALAS/AONS) in 20 mM Hepes, pH 7.5 containing 10% glycerol. For (A) – (C), AONS (--), ALAS (—), and ALAS/AONS (– · –).

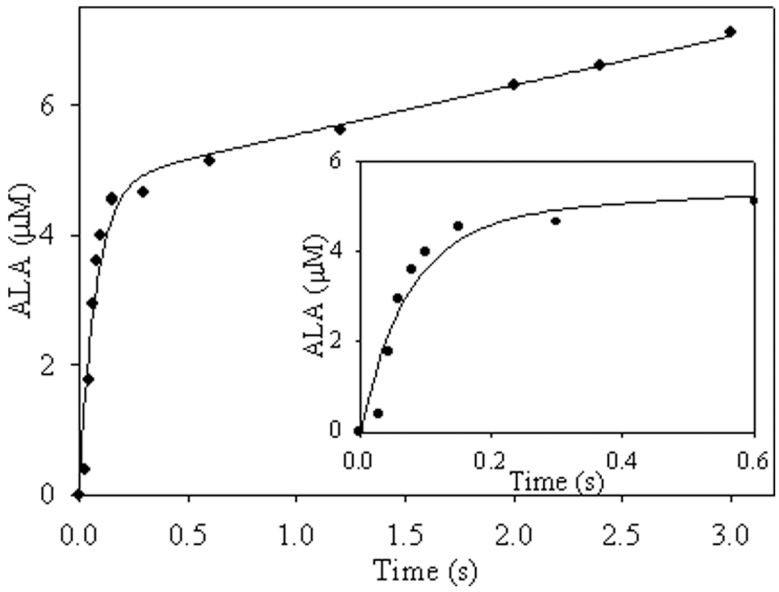

Figure 7. Kinetics of a pre-steady-state burst of ALA in the ALAS/AONS reaction

ALAS/AONS (50 μM) preincubated with glycine (140 mM) was quickly reacted with succinyl-CoA (150 μM) at 20 °C. The concentrations shown in *parentheses* are final concentrations after mixing. The reactions were quenched with perchloric acid (0.14 M) at various aging times, and the ALA concentration was determined. The *inset* illustrates the first 0.6 seconds of the reaction time course. The first 0.7 s of the time course is expanded while in the *inset* the time course is extended to 3.0 s. The curve represents the best fit to equation 1 with a burst amplitude of 4.7 ± 0.4 μM and a burst rate of 13.2 ± 2.6 s^{-1}.

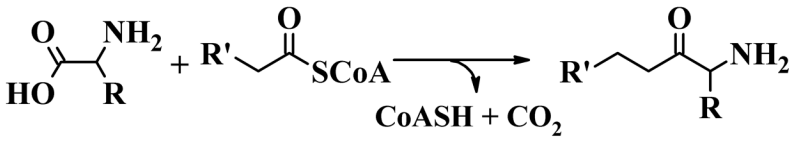

R = H and R' = $CH_2CO_2^-$ for ALAS
R = CH_3 and R' = $(CH_2)_4CO_2^-$ for AONS

Scheme 1.

Table 1

Nomenclature defining the plasmids and enzymes described in this report

Plasmid	Protein[a]	Description	Mass[b]	Reference
pGF23	ALAS	ALAS homodimer	56 kD	[26]
pTDT1	AONS	AONS homodimer	40 kD	This study
pGF27	ALAS^{K313A}	ALAS homodimer harboring the K313A mutation	56 kD	[27,37]
pTDT8	ALAS^{F341A}	ALAS homodimer harboring the F341A mutation	56 kD	This study
pAC1	ALAS/ALAS	Single polypeptide ALAS homodimer	112 kD	[23]
pCA1	ALAS^{K313A}/ALAS	Chimera of ALAS^{K313A} and ALAS	112 kD	This study
pMG1	ALAS/ALAS^{K313A}	Chimera of ALAS and ALAS^{K313A}	112 kD	This study
pTDT5	ALAS/AONS	Chimera of ALAS and AONS	96 kD	This study
pTDT4	AONS/ALAS	Chimera of AONS and ALAS	96 kD	This study
pTDT12	ALAS^{K313A}/AONS	Chimera of ALAS^{K313A} and AONS	96 kD	This study
pTDT17	AONS/ALAS^{K313A}	Chimera of AONS and ALAS^{K313A}	96 kD	This study
pTDT14	ALAS^{F341A}/AONS	Chimera of ALAS^{F341A} and AONS	96 kD	This study
pTDT15	AONS/ALAS^{F341A}	Chimera of AONS and ALAS^{F341A}	96 kD	This study
pTDT7	ALAS/AONS^{K236A}	Chimera of ALAS and AONS^{K236A}	96 kD	This study

[a] In the linked proteins the first abbreviation refers to the N-terminal enzyme.

[b] Monomeric molecular mass.

Table 2

Growth of transformed *E. coli* strains on selective media

		***E. coli* HU227**		***E. coli* R872**	
Plasmid	**Protein**	**LB/Amp/ALA**	**LB/Amp**	**LB/Amp**	**Biotin$^-$ minimal**
pGF23	ALAS	+	+	+	−
pTDT1	AONS	+	−	+	+
pGF27	ALAS^{K313A}	+	−	+	−
pTDT8	ALAS^{F341A}	+	−	+	−
pAC1	ALAS/ALAS	+	+	+	−
pCA1	ALAS^{K313A}/ALAS	+	+	+	−
pMG1	ALAS/ALAS^{K313A}	+	+	+	−
pTDT5	ALAS/AONS	+	+	+	+
pTDT4	AONS/ALAS	+	+	+	+
pTDT12	ALAS^{K313A}/AONS	+	−	+	+
pTDT17	AONS/ALAS^{K313A}	+	−	+	+
pTDT14	ALAS^{F341A}/AONS	+	−	+	+
pTDT15	AONS/ALAS^{F341A}	+	−	+	+
pTDT7	ALAS/AONS^{K236A}	+	+	+	−

Table 3

Summary of steady-state kinetic parameters for ALAS, ALAS/ALAS, ALAS/ALAS^{K313A} and ALAS^{K313A}/ALAS

	k_{cat} (min^{-1})	K_m^{Gly} (mM)	k_{cat}/K_m^{Gly} (min^{-1}mM^{-1})	K_m^{SCoA} (μM)	k_{cat}/K_m^{SCoA} (min^{-1}μM^{-1})	K_d^{ALA} (μM)
ALAS	10 ± 1[a]	23 ± 1[a]	0.43 ± 0.06[a]	2.3 ± 0.1[a]	4.3 ± 0.2[a]	25 ± 3[a]
ALAS/ALAS	55.4 ± 0.1[b]	16.7 ± 0.2[b]	3.32 ± 0.04[b]	0.45 ± 0.03[b]	123 ± 8[b]	1.46 ± 0.01
ALAS/ALAS^{K313A}	4.4 ± 0.2	11.8 ± 2.8	0.37 ± 0.09	1.8 ± 0.3	2.4 ± 0.4	6.8 ± 1.1
ALAS^{K313A}/ALAS	21.6 ± 0.7	14.8 ± 11.7	1.46 ± 0.17	0.32 ± 0.05	67.5 ± 10.8	2.3 ± 0.8

[a]Data from ref [28].

[b]Data from ref [23].

Table 4

ALAS activity: Summary of steady-state kinetic parameters for ALAS and ALAS/AONS chimera

	k_{cat} (min^{-1})	K_m^{Gly} (mM)	k_{cat}/K_m^{Gly} (min^{-1}mM^{-1})	K_m^{SCoA} (μM)	k_{cat}/K_m^{SCoA} (min^{-1}μM^{-1})
ALAS[a]	10 ± 1	23 ± 1	0.43 ± 0.02	2.3 ± 0.1	4.3 ± 0.2
ALAS/AONS	6.2 ± 0.8	5.5 ± 0.8	1.1 ± 0.2	1.5 ± 0.2	4.1 ± 0.7

[a]Data from ref [28]

Table 5

AONS activity: Summary of steady-state kinetic parameters for AONS and ALAS/AONS chimera

	k_{cat} (min^{-1})	$K_m^{Alanine}$ (mM)	$k_{cat}/K_m^{Alanine}$ (min^{-1}mM^{-1})	K_m^{PCoA} (μM)	k_{cat}/K_m^{PCoA} (min^{-1}μM^{-1})
AONS[a]	3.6 ± 0.6	0.5 ± 0.4	7.2 ± 1.3	25 ± 2	0.14 ± 0.03
ALAS/AONS	1.7 ± 0.3	0.25 ± 0.05	6.8 ± 1.8	10 ± 1	0.16 ± 0.03

[a]Data from ref [29]